International Journal of Pharmaceutics 367 (2009) 169–178

Contents lists available at ScienceDirect

International Journal of Pharmaceutics

journal homepage: www.elsevier.com/locate/ijpharm

Pharmaceutical Nanotechnology

Pulmonary drug delivery with aerosolizable nanoparticles in an *ex vivo* lung model

Moritz Beck-Broichsitter[a,b], Julia Gauss[b], Claudia B. Packhaeuser[a], Kerstin Lahnstein[b], Thomas Schmehl[b], Werner Seeger[b], Thomas Kissel[a], Tobias Gessler[b,*]

[a] *Department of Pharmaceutics and Biopharmacy, Philipps-University, Ketzerbach 63, D-35037 Marburg, Germany*
[b] *Medical Clinic II, Department of Internal Medicine, Justus-Liebig-University, Klinikstrasse 36, D-35392 Giessen, Germany*

ARTICLE INFO

Article history:
Received 23 July 2008
Received in revised form 5 September 2008
Accepted 9 September 2008
Available online 19 September 2008

Keywords:
Nanoparticles
Biodegradable branched polyesters
Nebulization
Isolated lung
Pulmonary drug delivery
Targeting

ABSTRACT

The use of colloidal carrier systems for pulmonary drug delivery is an emerging field of interest in nanomedicine. The objective of this study was to compare the pulmonary absorption and distribution characteristics of the hydrophilic model drug 5(6)-carboxyfluorescein (CF) after aerosolization as solution or entrapped into nanoparticles in an isolated rabbit lung model (IPL). CF-nanoparticles were prepared from a new class of biocompatible, fast degrading, branched polyesters by a modified solvent displacement method. Physicochemical properties, morphology, encapsulation efficiency, *in vitro* drug release, stability of nanoparticles to nebulization, aerosol characteristics as well as pulmonary dye absorption and distribution profiles after nebulization in an IPL were investigated.

CF-nanoparticles were spherical in shape with a mean particle size of 195.3 ± 7.1 nm, a polydispersity index of 0.225 ± 0.017 and a ζ-potential of -28.3 ± 0.3 mV. Encapsulation efficiencies of CF were as high as about 60% (drug loading of 3% (w/w)); 90% of the entrapped CF were released during the first 50 min *in vitro*. Nanoparticle characteristics were not significantly affected by the aerosolization process utilizing a vibrating mesh nebulizer. After deposition of equal amounts of CF in the IPL, less CF was detected in the perfusate for CF-nanoparticles (plateau concentration 9.2 ± 2.4 ng/ml) when compared to CF aerosolized from solution (17.7 ± 0.8 ng/ml).

In conclusion, the data suggest that inhalative delivery of biodegradable nanoparticles may be a viable approach for pulmonary drug delivery. Moreover, a targeting effect to the lung tissue is claimed.

1. Introduction

Pulmonary drug delivery offers several advantages in the treatment of respiratory diseases over other routes of administration. Inhalation therapy enables the direct application of a drug within the lungs. The local pulmonary deposition and delivery of the administered drug facilitates a targeted treatment of respiratory diseases, such as pulmonary arterial hypertension (PAH), without the need for high dose exposures by other routes of administration (Badesch et al., 2004). The intravenous application of short acting vasodilators has been the therapy of choice for patients with PAH over the past decade (McLaughlin et al., 2002). The relative severity of side effects led to the development of new prostacyclin analogues and alternative routes of administration (Rich and McLaughlin, 1999). One such analogue, iloprost (Ventavis®), is a worldwide approved therapeutic agent for treatment of PAH (Olschewski et al., 2002). Inhalation of this compound is an attractive concept minimizing the side effects by its pulmonary selectivity (Gessler et al., 2001). Unfortunately, the short half life of iloprost requires frequent inhalation manoeuvres, ranging up to 9 times a day (Gessler et al., 2008). Therefore, an aerosolizable controlled release formulation would improve a patient's convenience and compliance.

Controlled drug delivery systems have become increasingly attractive options for inhalation therapies. A large number of carrier systems have been developed and investigated as potential controlled drug delivery formulations to the lung, including drug loaded lipid and polymer based particles (Zeng et al., 1995). Among the various drug delivery systems considered for pulmonary application, nanoparticles demonstrate several advantages for the treatment of respiratory diseases, like prolonged drug release, cell specific targeted drug delivery or modified biological distribution of drugs, both at the cellular and organ level (Pison et al., 2006; Sung et al., 2007; Azarmi et al., 2008; Yang et al.,

* Corresponding author. Tel.: +49 641 99 42453; fax: +49 641 99 42489.
E-mail address: tobias.gessler@innere.med.uni-giessen.de (T. Gessler).

0378-5173/$ – see front matter © 2008 Elsevier B.V. All rights reserved.
doi:10.1016/j.ijpharm.2008.09.017

2008). Nanoparticles composed of biodegradable polymers show assurance in fulfilling the stringent requirements placed on these delivery systems, such as ability to be transferred into an aerosol, stability against forces generated during aerosolization, biocompatibility, targeting of specific sites or cell populations in the lung, release of the drug in a predetermined manner, and degradation within an acceptable period of time (Rytting et al., 2008).

In order to combine the advantages of the direct access to the lung via inhalation with the unique properties of nanotechnology, the authors designed and characterized *in vitro* different nanocarrier systems for aerosol application, such as biodegradable nanoparticles (Dailey et al., 2003a,b). The most promising nanoparticle preparation has been formulated from a hydrophilic poly(lactide-*co*-glycolide) (PLGA) derivative, composed of short PLGA chains grafted onto an amine-substituted poly(vinyl alcohol) backbone, namely poly[vinyl 3-(diethylamino)propylcarbamate-*co*-vinyl acetate-*co*-vinyl alcohol]-*graft*-poly(D,L-lactide-*co*-glycolide), abbreviated as DEAPA. The amphiphilic properties of DEAPA make it highly suited for pulmonary formulations in several ways. On the one hand the flexibility of this type of polymer was shown through modifications in the degree of amine substitution and PLGA chain length, especially with regard to the controlled variability of biodegradation rates (Unger et al., 2008) and *in vitro* cytotoxicity (Unger et al., 2007). Moreover, this type of biodegradable polyester revealed no signs of inflammatory response *in vivo* (Dailey et al., 2006). On the other hand nanoparticles can be generated from DEAPA without the use of additional surfactant stabilizers. Furthermore, it has been reported that the addition of varying amounts of a polyanionic excipient, such as dextrane sulfate or carboxymethyl cellulose (CMC), to the polymer during nanoparticle formulation can generate nanoparticles of variable physicochemical properties. This attribute was used to design nanoparticle systems with greater stability in the face of shear forces and adjustable nanoparticle alveolar epithelial cell interactions (Dailey et al., 2003a).

Different methods are used to assess the behaviour of pulmonary administered drug loaded delivery systems ranging from *in vitro* to *in vivo* systems (Sakagami, 2006). *Ex vivo* isolated, perfused and ventilated lung models have been utilized in numerous pharmacological and toxicological studies to elucidate the fate of inhaled drug or toxic substances (Ewing et al., 2006, 2008).

The purpose of the present study was to compare the pulmonary absorption and distribution characteristics of the hydrophilic model drug 5(6)-carboxyfluorescein (CF) after aerosolization as solution or entrapped into nanoparticles in an isolated, perfused and ventilated rabbit lung model (IPL). The preparation method of nanoparticles made up of a promising new class of biocompatible, fast degrading, branched polyester (DEAPA) loaded with CF by a modified solvent displacement technique is described. The particle size, particle size distribution, ζ-potential, particle morphology, drug encapsulation efficiency and *in vitro* drug release of the prepared CF loaded DEAPA nanoparticles were investigated using photon correlation spectroscopy (PCS), laser Doppler anemometry (LDA), atomic force microscopy (AFM) and fluorescence spectroscopy. Furthermore, the stability of the nanoparticles to the nebulization procedure utilizing an actively vibrating mesh device (Aeroneb® Professional) was determined using the above mentioned techniques. The aerosol characteristics of both formulations were analyzed by laser light scattering. Finally, the pulmonary dye absorption profiles for the two formulations after nebulization in an IPL were compared by monitoring the CF concentration in the perfusate over the time. Additionally, the dye distributions in the different compartments of the IPL at the end of the experiments were also evaluated.

2. Materials and methods

2.1. Materials

The biocompatible, fast degrading, branched polyester, namely poly[vinyl 3-(diethylamino)propylcarbamate-*co*-vinyl acetate-*co*-vinyl alcohol]-*graft*-poly(D,L-lactide-*co*-glycolide), synthesized and characterized as described earlier by Wittmar et al. (2006) was used as polymeric nanoparticle matrix material. These polyesters were specifically designed for drug delivery to the lung and are comprised of short poly(D,L-lactide-*co*-glycolide) (PLGA) chains grafted onto an amine-substituted poly(vinyl alcohol) (PVA) backbone. As abbreviation A(x) – y is used. A is the abbreviation of the type of amine substitution (DEAPA = 3-diethylamino-1-propylamin), x is the total average number of amine functions on the PVA backbone, and y the PLGA side chain length. In this study DEAPA(39)-10 was used with the molecular structure depicted in Fig. 1. Carboxymethyl cellulose (CMC) (Tylopur® C 600) was purchased from Clariant (Sulzbach, Germany). The pharmacologically inert fluorescent dye 5(6)-carboxyfluorescein (CF) (Fluka, Buchs, Switzerland) was chosen as a water soluble model drug. Alveofact® was a gift from Boehringer Ingelheim (Ingelheim, Germany). All other chemicals and solvents used in this study were of the highest analytical grade commercially available.

2.2. Methods

2.2.1. Preparation of dye solution

The dye solution containing CF was prepared in isotonic phosphate-buffered saline (PBS) at pH 7.4 to yield a final concentration of 50 μg/ml.

2.2.2. Preparation of nanoparticles

CF loaded nanoparticles were prepared by a modified solvent displacement technique, that has been described in detail

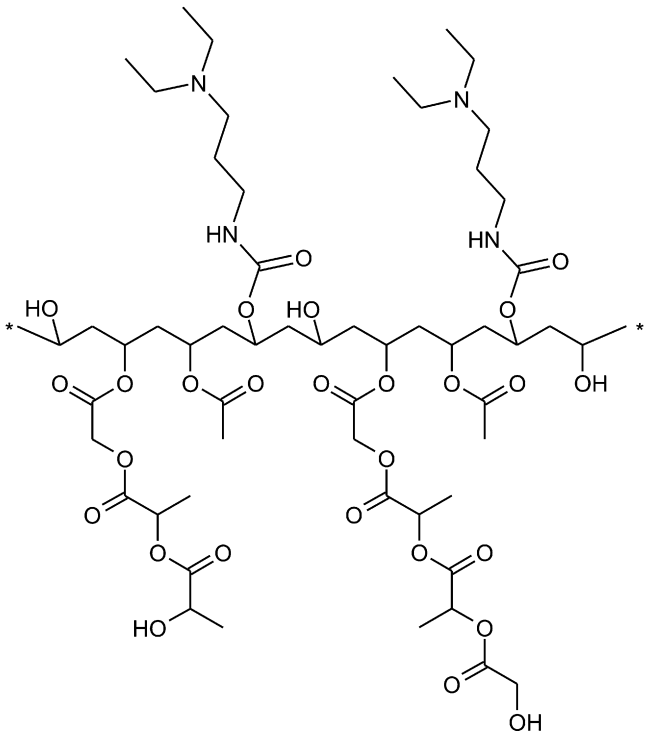

Fig. 1. Structure of the polymer used in this study: DEAPA(39)-10.

elsewhere (Jung et al., 2000). To avoid artificial surfactants, the preparation was modified in the following manner: 5.0 mg of DEAPA(39)-10 was dissolved in 1 ml of acetone at 25 °C. In addition CF was dissolved in acetone to add up to a final concentration of 500 μg/ml. 1 ml of the polymer stock solution (5.0 mg/ml) was mixed vigorously with 0.5 ml of the CF stock solution (500 μg/ml). The resulting solution was subsequently injected into a magnetically stirred (500 rpm) aqueous phase of 5 ml of filtrated and double distilled water (pH 7.0, conductance 0.055 μS/cm, 25 °C) containing 50 μg CMC/mg DEAPA(39)-10 according to the findings of Dailey et al. (2003a) using a special apparatus. The apparatus consists of an electronically adjustable single-suction pump which was used to inject the organic solution into the aqueous phase through an injection needle (Fine-Ject® 0.6 × 30 mm) at a constant flow rate (8.0 ml/min). The pump rate was regulated and constantly monitored by electric power control. After injection of the organic phase, the resulting colloidal suspension was stirred for ~3 h under reduced pressure to remove the organic solvent. Particles were characterized and used directly after preparation.

2.2.3. Physicochemical characterization of nanoparticles

2.2.3.1. Particle size measurement. The average particle size and size distribution of the obtained nanoparticles were determined by photon correlation spectroscopy (PCS) using a Zetasizer NanoZS/ZEN3600 (Malvern Instruments, Herrenberg, Germany). The analysis was performed at a temperature of 25 °C using samples appropriately diluted with filtrated and double distilled water in order to avoid multiscattering events. The DTS V. 5.02 software was used to calculate particle mean diameter (Z-Ave) and the width of the fitted Gaussian distribution, which is displayed as the polydispersity index (PDI). Each size measurement was performed with at least 10 runs. All measurements were carried out in triplicate directly after nanoparticle preparation.

2.2.3.2. ζ-Potential measurement. The ζ-potential was measured by laser Doppler anemometry (LDA) using a Zetasizer NanoZS/ZEN3600 (Malvern Instruments, Herrenberg, Germany). The analysis was performed at a temperature of 25 °C using samples appropriately diluted with 1.54 mM NaCl solution in order to maintain a constant ionic strength. The DTS V. 5.02 software was used to calculate the average ζ-potential values from the data of multiple runs. All measurements were carried out in triplicate directly after nanoparticle preparation.

2.2.4. Atomic force microscopy

Morphology of nanoparticles was analyzed by atomic force microscopy (AFM). Samples were prepared by placing a sample volume of 10 μl onto commercial glass slides (RMS < 3 nm). The slides were incubated with the nanoparticle suspension for 10 min before washing twice with distilled water and drying in a stream of dry nitrogen. Samples were investigated within 2 h after preparation. AFM was performed using a NanoWizard® (JPK Instruments, Berlin, Germany) in intermittent contact mode to avoid damage to the sample surface. Commercially available Si_3N_4 tips attached to I-type cantilevers with a length of 230 μm and a nominal force constant of 40 N/m (NSC16 AlBS, Micromasch, Tallinn, Estonia) were used. The scan frequency was between 0.5 and 1 Hz and antiproportional to the scan size. The results were visualized as trace signal in amplitude mode.

2.2.5. Determination of entrapped CF

The encapsulation efficiency was calculated indirectly by determining the remaining concentration of CF in the supernatant after centrifugation. Samples of 175 μl were subjected to ultracentrifugation (Airfuge®, Beckman Coulter, Krefeld, Germany) at 110,000 rpm (199,000 × *g*) for 20 min at 4 °C. The supernatant containing the dissolved free model drug CF was used to determine the concentration by fluorescence spectroscopy. The amount of entrapped CF was calculated as relative encapsulation efficiency from the supernatant (CF_{sup}) after centrifugation to the total amount of CF (CF_{tot}) using the following equation:

$$\text{Encapsulation efficiency } (\%) = 100 - \frac{CF_{sup} \cdot 100}{CF_{tot}}$$

2.2.6. In vitro release studies

The *in vitro* drug release studies were carried out in PBS pH 7.4 and Alveofact® (0.5 mg/ml in PBS pH 7.4), respectively, over a 240 min period of time, according to the run-time of the experiments with the isolated, perfused and ventilated rabbit lung model. The studies were performed with nanoparticles containing 5% (w/w) theoretical CF loading. Samples of the nanoparticle suspensions (0.4 ml) were transferred to 15 ml plastic tubes and diluted with the release medium resulting in a volume of 10 ml. Incubation occurred at 37 °C while undergoing vertical rotation (20 rpm) (Rotatherm®, Gebr. Liebisch, Bielefeld, Germany). Samples of 175 μl were taken at predetermined time points and centrifuged prior to further determining the cumulative release of CF by fluorescence spectroscopy. In parallel, nanoparticle suspensions without CF and pure CF were incubated in the release medium under the same conditions to exclude background fluorescence caused by the polymer or loss of CF during incubation time, respectively.

2.2.7. Isolated, perfused and ventilated lung model (IPL)

The isolated, perfused and ventilated lung model has been previously described (Seeger et al., 1994). Briefly, male rabbits weighing 2.5–3.5 kg were gradually anesthetized with a mixture of ketamine (Ketavet®, Pharmacia, Erlangen, Germany) and xylazine (Rompun®, Bayer Vital, Leverkusen, Germany) in a ratio of 3 to 2 and anticoagulated with heparin (1000 U/kg). After achieving a deep anesthetization the animals were ventilated with room air via a tracheal cannula using a Harvard respirator (cat/rabbit Ventilator, Hugo Sachs Elektronik, March Hugstetten, Germany). Catheters were inserted into the left atrium and the pulmonary artery after a midsternal thoracotomy. Perfusion with ice-cold Krebs-Henseleit buffer (Serag-Wiessner, Naila/Bayern, Germany) with a pulsatile flow of 10–20 ml/min was immediately started. The lungs were removed from the thorax and placed in a temperature equilibrated chamber at 4 °C, freely suspended from a force transducer for monitoring the lung weight. Then the perfusion flow was slowly increased to 100 ml/min. At the same time the temperature of the perfusion fluid and the housing chamber was raised to 39 °C. After a 30 min steady-state period, the perfusion fluid was exchanged once by fresh buffer (total volume 345 ml). With the onset of artificial perfusion an air mixture of 21% O_2, 5.3% CO_2, and 73.7% N_2 was used for ventilation (tidal volume 30 ml, frequency 30 strokes/min). A positive end-expiratory pressure of 1 cmH_2O was used throughout. Pulmonary arterial pressure (PAP), pulmonary venous pressure (PVP, measured in the left atrium), inflation pressure, and the weight of the isolated lung were registered continuously. Left atrial pressure was set 1.5 mmHg in all experiments. Only those lungs were selected for the study that fulfilled three criteria: firstly homogeneous white appearance with no signs of haemostasis, oedema, or atelectasis; secondly a pulmonary artery and ventilation pressure in the normal range; and thirdly no weight gain during the steady-state period. Usually, sampling, evaporation and fluid dripping caused losses of perfusate during the experiments (in total ~50 ml/240 min). The perfusate drops which escaped from the whole surface of the lungs (~6 ml/240 min) were collected and analyzed.

2.2.8. Nanoparticle stability during nebulization

To study the stability of CF loaded DEAPA(39)-10 nanoparticles during nebulization a actively vibrating mesh nebulizer (Aeroneb® Professional, Aerogen Inc., Dangan, Galway, Ireland) was used. The collection of the nebulized nanoparticle suspension and the investigation of nanoparticle stability were performed as previously described (Dailey et al., 2003a). Briefly, samples of 3 ml suspension were aerosolized at an airflow rate of 10 l/min to exhaustive nebulization of the reservoir. Samples of the nebulized aerosol were collected by placing a glass microscopic slide in front of the nebulizer T-shaped mouthpiece and allowing the aerosol droplets to deposit on the glass. The resulting condensation fluid was collected for further analysis. The stability of the nebulized nanoparticle suspensions was investigated using PCS, LDA and AFM. In addition, the amount of encapsulated CF of the aerosolized nanoparticles was quantified as described above.

2.2.9. Aerosol particle size determination by laser diffraction

For aerosolization the actively vibrating mesh nebulizer Aeroneb® Professional was employed. In order to compare particle size distribution of the two aerosolized formulations and NaCl 0.9% (m/V) as control, the mass median aerodynamic diameters (MMAD) of the aerosol droplets were determined using laser light scattering (HELOS, Sympatec, Clausthal-Zellerfeld, Germany). The measurements (six runs of 100 × 50 ms duration each) were performed with an additional air flow rate of 10 l/min through the T-shaped mouthpiece of the Aeroneb® Professional nebulizer. Furthermore, the aerosol particle size was investigated at the entrance of the inspiratory tubing system to the trachea of the lung (① in Fig. 2) with the Aeroneb® Professional connected to the inspiratory system between the ventilator and the end of the inspiration tubing. All data were analyzed in Mie mode. The density of the nebulized solution was set equal to unit density and thus the measured volume median diameter (VMD) equalled the MMAD. The geometric standard deviation (GSD) was calculated from the laser diffraction values according to the following equation:

$$\mathrm{GSD} = \sqrt{\frac{84\%\ \text{undersize}}{16\%\ \text{undersize}}}$$

2.2.10. Aerosol output and lung deposition

The total aerosol output was determined gravimetrically by weighing the nebulizer (Aeroneb® Professional) before and after each nebulization experiment. The resulting difference in weight was used to calculate the aerosol output rate in g/min.

The amount of aerosol deposited in the IPL was examined in separate experiments using ^{99m}Tc-enriched saline. ^{99m}Tc (10–14 MBq, Department of Nuclear Medicine, Universitaetsklinikum Giessen und Marburg GmbH, Germany) was dissolved in 10 ml saline and 3 ml of this solution were nebulized with the Aeroneb® Professional for approximately 5 to 7 min into the lung. In order to prevent diffusion of deposited ^{99m}Tc into the perfusate, the lung was clamped and perfusion was stopped during aerosol delivery. After nebulization, the lung was immediately removed from the system and the radioactivity of the lung (lung deposition) and the expiratory filter (exhaled fraction) were measured by a gamma-counter (Raytest, Straubenhardt, Germany). The deposition fraction (DF) was calculated as follows:

$$\mathrm{DF} = \frac{\mathrm{LD}}{\mathrm{IF}} = \frac{\mathrm{LD}}{\mathrm{LD} + \mathrm{EF}}$$

where LD is the lung deposition, EF the exhaled fraction, and IF is the inhaled fraction = LD + EF.

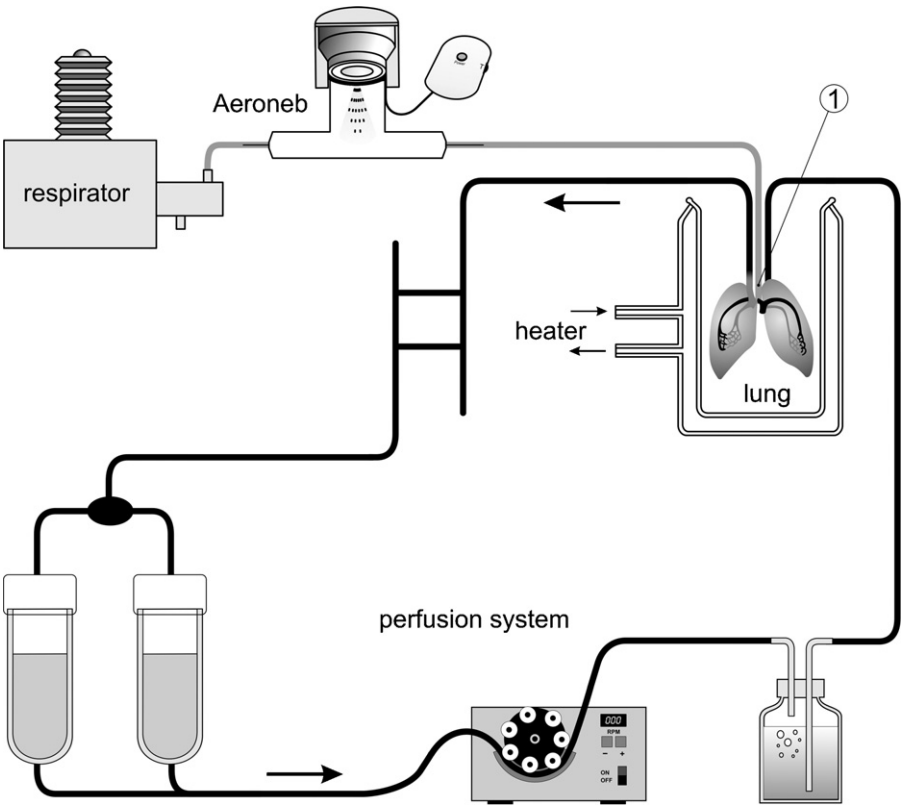

Fig. 2. Schematic of the isolated, perfused and ventilated rabbit lung model as used for absorption studies of 5(6)-carboxyfluorescein in this study ("1": site for the determination of the formulation aerosols MMAD and GSD at the entrance of the inspiratory tubing system to the trachea of the lung).

2.2.11. Pulmonary absorption and distribution characteristics of nebulized CF formulations in the IPL

A detailed description of the IPL as used for the pulmonary absorption and distribution experiments of 5(6)-carboxyfluorescein in this study can be found elsewhere (Lahnstein et al., 2008). A schematic of the IPL is depicted in Fig. 2. Briefly, for aerosol delivery of the two formulations the Aeroneb® Professional was connected to the inspiratory tubing between the ventilator and the rabbit lung to be passed through by the inspiration gas. Three millilitres of either the CF solution (50 μg/ml) or the nanoparticle suspension containing a total CF amount of 50 μg/ml were nebulized for approximately 5–7 min into the IPL. In order to determine the CF perfusate concentrations, 800 μl samples were taken from the venous part of the system. The sampling interval was every 10 min up to 240 min. Additionally, the dye concentration in the collected perfusate drops and the amount of fluorescent dye remaining in the lung lining fluid were determined. Therefore, the lung was lavaged with a total of 150 ml of fresh perfusion fluid at the end of the experiment. A 50 ml fraction was intratracheally instilled and reaspirated three times. The total recovery of lavage fluid was 80–95%. Before measurement, the lavage and the dripping fluid were centrifuged at 300 × *g* for 10 min to remove cells. The fluorescence caused by CF in the samples was determined by fluorescence spectroscopy.

In order to consider loss of perfusate during the experiments the measured fluorescent concentration was corrected by the following formula:

$$c_{\mathrm{corr}}(t) = \frac{c(t)V_{\mathrm{p}}(t) + [V_{\mathrm{p}}(0) - V_{\mathrm{p}}(t)]c(t)/2}{V_{\mathrm{p}}(0)} = \frac{c(t)}{2}\left[\frac{V_{\mathrm{p}}(t)}{V_{\mathrm{p}}(0)} + 1\right]$$

where $c_{\mathrm{corr}}(t)$ is the corrected dye concentration in perfusate after time t, $c(t)$ the measured dye concentration in perfusate after time t, $V_{\mathrm{p}}(t)$ the perfusate volume after time t, and $V_{\mathrm{p}}(0)$ is the perfusate volume at the beginning.

The pharmacokinetic parameters, i.e. the time until a stable plateau was accomplished (t_{max}), the plateau concentration (c_{max}), the half time to reach the plateau concentration ($t_{½}$) and the concentration at $t_{½}$ ($c_{½}$), for both formulations delivered to the IPL were calculated from the obtained perfusate concentration–time profiles. In addition the mean residence time (MRT) of CF in the lung was calculated (Dost, 1958) and is given by the following equation:

$$\mathrm{MRT} = \frac{\mathrm{ABC}}{M(t_{\mathrm{max}})}$$

where ABC is the area between the curve and the line through c_{max}, and $M(t_{\mathrm{max}})$ the amount of CF in the perfusate after reaching a stable perfusate plateau concentration.

2.2.12. CF quantification by fluorescence spectroscopy

Samples collected from freshly prepared nanoparticle suspensions, during the release or the nanoparticle nebulization stability experiments, respectively, were centrifuged as described above to separate the free from the incorporated model drug CF. The supernatants containing the dissolved free model drug were diluted with Tris 0.1 M (pH 8) to reach a CF concentration between 2 and 50 ng/ml. Samples from the IPL were collected, centrifuged as described above and analyzed for fluorescence intensity without further treatment. The concentration of CF in the samples was determined using a fluorescence plate reader (FL600, Bio-Tek, Bad Friedrichshall, Germany) equipped with the following filter: λ_{ex}: 485/20, λ_{em}: 530/25. 100 μl of each sample were placed in 96-well plates (Costar, Cambridge, USA) and the fluorescence intensity was measured immediately. The CF content was calculated using a calibration curve. The linearity range of CF is found to be between 2 and 50 ng/ml ($R^2 = 0.9995$). Care was taken to protect the samples from light throughout the experiments.

2.2.13. Statistics

All measurements were carried out in triplicates and values are presented as the mean ± S.D. unless otherwise noted. Statistical calculations were carried out using the software SigmaStat 3.5 (STATCON, Witzenhausen, Germany). To identify statistical significant differences, the non-parametric Mann–Whitney rank sum test was performed. Probability values of $p < 0.05$ were considered significant.

3. Results

3.1. Nanoparticle characteristics

The measured physicochemical characteristics of the CF loaded DEAPA(39)-10 are summarized in Table 1. A representative AFM image of the freshly prepared nanoparticles is shown in Fig. 3a). Freshly prepared nanoparticles were of spherical shape with a mean particle size of 195.3 ± 7.1 nm (mean ± S.D., $n = 4$), a polydispersity index of 0.225 ± 0.017 (mean ± S.D., $n = 4$) and a ζ-potential of −28.3 ± 0.3 mV (mean ± S.D., $n = 4$), respectively. The preparation method assured an encapsulation efficiency of CF in the DEAPA(39)-10 nanoparticles of 59.4 ± 2.5% (mean ± S.D., $n = 4$), resulting in a drug loading of 2.97 ± 0.13% (w/w) (mean ± S.D., $n = 4$).

3.2. In vitro release studies

The *in vitro* release profile of the nanoparticle preparations is depicted in Fig. 4. In both release media, PBS pH 7.4 and Alveofact®, respectively, a pronounced burst effect was detected. During the first 50 min of incubation 90% of the encapsulated CF was released, followed by a negligible release for 3 h. Background fluorescence caused by the polymer or loss of CF during incubation time, respectively, was not detected.

3.3. Nanoparticle stability during nebulization

The results from the investigation of CF loaded DEAPA(39)-10 nanoparticles after nebulization utilizing the Aeroneb® Professional are shown in Table 1. The nanoparticles were spherical (Fig. 3 b)) with a mean particle size of 185.9 ± 4.4 nm (mean ± S.D., $n = 4$), a polydispersity index of 0.214 ± 0.015 (mean ± S.D., $n = 4$) and a ζ-potential of −30.9 ± 1.9 mV (mean ± S.D., $n = 4$), respectively.

Table 1
Properties of CF loaded DEAPA(39)-10 nanoparticles before and after nebulization with the vibrating mesh nebulizer Aeroneb® Professional.

Nanoparticles	Size (nm)	Polydispersity Index	ζ-Potential (mV)	Encapsulation efficiency (%)
Freshly prepared	195.3 ± 7.1	0.225 ± 0.017	−28.3 ± 0.3	59.4 ± 2.5
Nebulized	185.9 ± 4.4	0.214 ± 0.015	−30.9 ± 1.9	62.2 ± 4.5

Values are presented as the mean ± S.D.
$n = 4$.
No statistically significant differences were observed between the sample values.

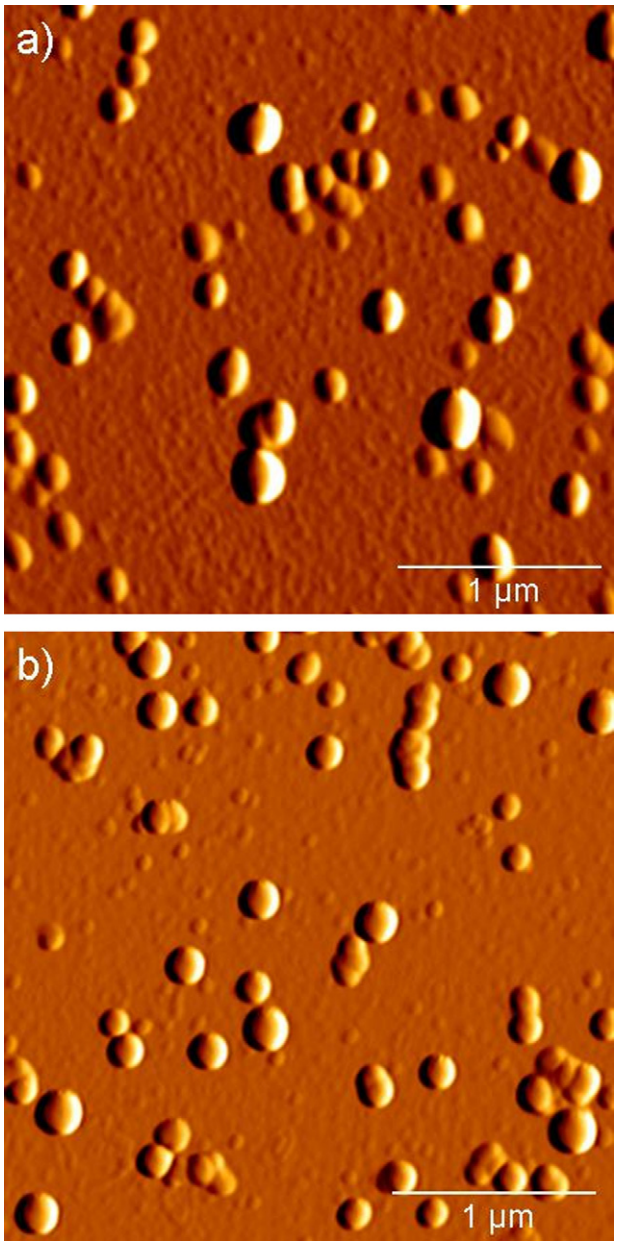

Fig. 3. Representative AFM images of 5(6)-carboxyfluorescein loaded DEAPA(39)-10 nanoparticles; (a) freshly prepared and (b) after nebulization with the vibrating mesh nebulizer Aeroneb® Professional.

The determined value for the encapsulation efficiency of CF in the DEAPA(39)-10 nanoparticles after nebulization was 62.2 ± 4.5% (mean ± S.D., $n = 4$), resulting in a drug loading of 3.11 ± 0.23% (w/w) (mean ± S.D., $n = 4$). No statistically significant differences were found between the values for freshly prepared and aerosolized nanoparticles.

3.4. Aerosol particle size distribution

The mean MMAD and GSD of the aerosolized saline and both CF formulations are presented in Fig. 5. MMAD was 5.12 ± 0.16 µm (mean ± S.D., $n = 3$) for NaCl 0.9%, 5.48 ± 0.32 µm (mean ± S.D., $n = 3$) for CF solution and 5.35 ± 0.20 µm (mean ± S.D., $n = 3$) for the CF loaded DEAPA(39)-10 nanoparticle formulation with a statistically significant difference between NaCl 0.9% and CF solution as well as between NaCl 0.9% and CF loaded DEAPA(39)-10 nanoparticle formulation ($p < 0.005$). GSD was 2.05 ± 0.09 (mean ± S.D., $n = 3$) for NaCl 0.9%, 2.13 ± 0.12 (mean ± S.D., $n = 3$) for CF solution and 1.91 ± 0.06 (mean ± S.D., $n = 3$) for the CF loaded DEAPA(39)-10 nanoparticle formulation with a statistically significant difference between NaCl 0.9% and CF solution ($p < 0.005$) as well as between NaCl 0.9% and CF loaded DEAPA(39)-10 nanoparticle formulation ($p < 0.05$). The mean MMAD and GSD of NaCl 0.9% at the entrance of the inspiratory tubing system to the trachea of the lung ("1" in Fig. 2) are also given as NaCl 0.9% (IPL) in Fig. 5. The MMAD was 3.12 ± 0.13 µm (mean ± S.D., $n = 3$) and the GSD was 1.69 ± 0.06 (mean ± S.D., $n = 3$). Both values are statistically significant different compared with the values for NaCl 0.9% ($p < 0.005$).

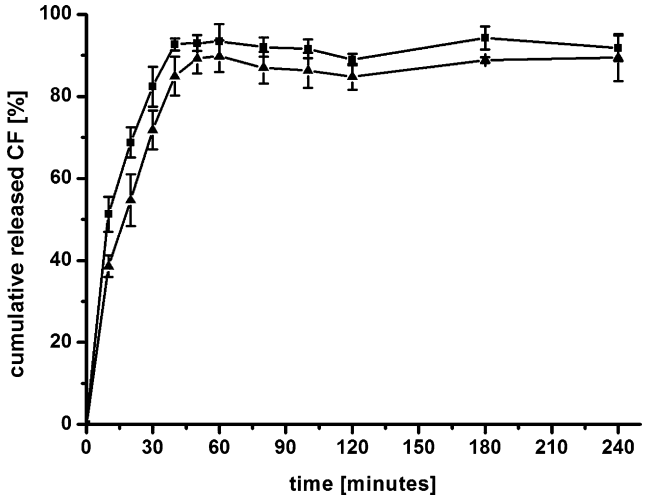

Fig. 4. Release characteristics of DEAPA(39)-10 nanoparticles loaded with 5(6)-carboxyfluorescein (CF) in PBS pH 7.4 (■) and Alveofact® (▲), respectively. Values are presented as the mean ± S.D. ($n = 4$).

3.5. Aerosol output and lung deposition

The total aerosol output, determined gravimetrically by weighing the nebulizer before and after exhaustive nebulization of the reservoir, and aerosol output rate amounted to 2.67 ± 0.12 g and 0.56 ± 0.01 g/min for NaCl 0.9%, 2.75 ± 0.21 g and 0.55 ± 0.01 g/min for CF solution, 2.72 ± 0.14 g and 0.44 ± 0.08 g/min for the CF loaded

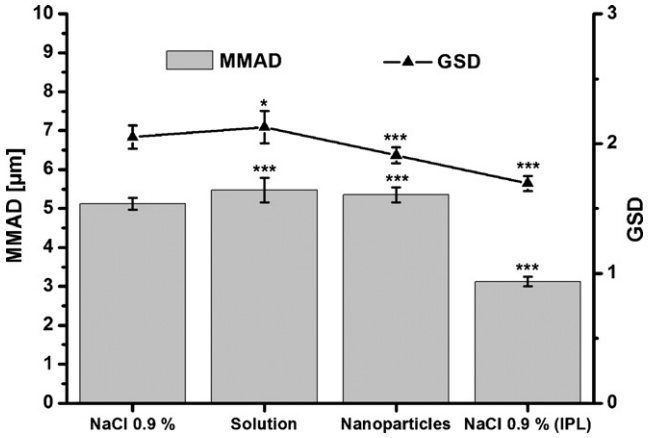

Fig. 5. Particle sizes (MMAD) and geometric standard deviation (GSD) of the aerosolized 5(6)-carboxyfluorescein formulations in comparison to NaCl 0.9%. The MMAD and GSD of NaCl 0.9% at the entrance of the inspiratory tubing system to the trachea of the lung ("1" in Fig. 2) is also given as NaCl 0.9% (IPL). Values are presented as the mean ± S.D. ($n = 3$). The asterisks denote statistically significant differences compared to NaCl 0.9% (* $p < 0.05$; *** $p < 0.005$).

Table 2
Pharmacokinetic parameter estimates of both formulation exposures to the isolated, perfused and ventilated rabbit lung model.

Formulation	t_{max} (min)	c_{max} (ng/ml)	$t_{½}$ (min)	$c_{½}$ (ng/ml)	MRT (min)
Solution	140.0 ± 10.0	17.7 ± 0.8	29.6 ± 9.6	8.8 ± 0.4	38.9 ± 11.1
Nanoparticles	140.0 ± 10.0	9.2 ± 2.4	38.8 ± 2.1	4.6 ± 1.2	46.6 ± 4.6

Values are presented as the mean ± S.D.
$n = 3$ for each formulation.

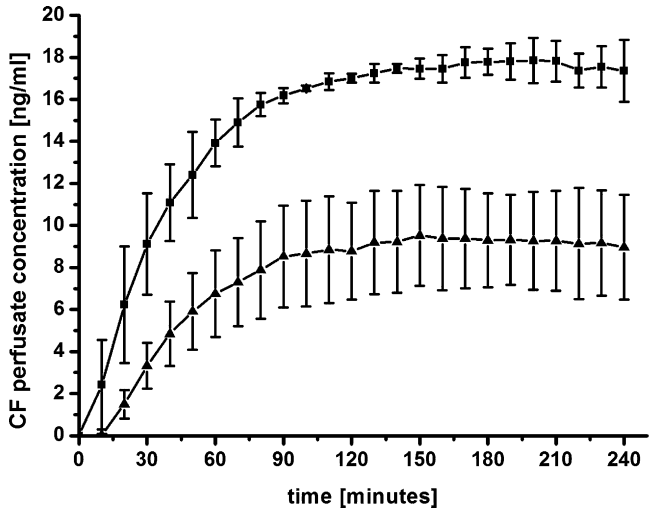

Fig. 6. Perfusate concentration–time profiles of 5(6)-carboxyfluorescein (CF) in the isolated, perfused and ventilated rabbit lung model after nebulization of 3 ml of CF solution (50 μg/ml) (■) and 3 ml of DEAPA(39)-10 nanoparticle suspension loaded with CF (50 μg/ml) (▲), respectively. Values are presented as mean ± S.D. ($n = 3$ for each formulation).

DEAPA(39)-10 nanoparticle formulation (mean ± S.D., $n = 3$ for all measurements). No statistically significant difference was seen for the aerosol output rates of both formulations compared to NaCl 0.9%. Lung deposition, as assessed by nebulization of ^{99m}Tc-enriched saline, was 0.37 ± 0.03 ml (mean ± S.D., $n = 3$). In the expiratory filter 0.16 ± 0.01 ml (mean ± S.D., $n = 3$) were found and therefore the deposition fraction was calculated to 70.0 ± 0.2% (mean ± S.D., $n = 3$).

3.6. Pulmonary absorption and distribution characteristics of nebulized CF formulations in the IPL

Fig. 6 shows the concentration–time profiles of CF in the perfusate following the pulmonary administration by inhalation. The perfusate concentration–time profiles for CF solution and CF loaded DEAPA(39)-10 nanoparticles showed similar characteristics with regard to the curve progression. After a continuous increase in CF perfusate concentration a plateau concentration was accomplished. The absorption degree of CF from nanoparticles by the IPL was less than those of CF from solution denoted by a lower plateau concentration in the perfusate.

Table 2 summarizes the pharmacokinetic parameters for both formulation exposures to the IPL. After 140 ± 10.0 min (mean ± S.D., $n = 3$) of continuous increase in CF perfusate concentration a stable plateau of 17.7 ± 0.8 ng/ml (mean ± S.D., $n = 3$) was reached for the CF released from solution. CF loaded DEAPA(39)-10 nanoparticles showed an increasing CF perfusate concentration for the first 140.0 ± 10.0 min (mean ± S.D., $n = 3$). The resulting steady-state concentration was 9.2 ± 2.4 ng/ml (mean ± S.D., $n = 3$). The MRT of CF in the lung from solution and nanoparticles was estimated to be 38.9 ± 11.1 min (mean ± S.D., $n = 3$) and 46.6 ± 4.6 min (mean ± S.D., $n = 3$), respectively.

The final CF distribution within the experimental system is given in Table 3. After administration of aerosolized CF solution to the IPL a total of 7042 ± 517 ng (mean ± S.D., $n = 3$) CF was recovered with 5110 ± 355 ng (mean ± S.D., $n = 3$) in the perfusate and 1093 ± 361 ng (mean ± S.D., $n = 3$) in the lavage fluid. A lower recovery of only 3923 ± 1127 ng (mean ± S.D., $n = 3$) was measured in the experiments with administration of aerosolized CF loaded DEAPA(39)-10 nanoparticle to the IPL with 2365 ± 519 ng (mean ± S.D., $n = 3$) in the perfusate and 878 ± 161 ng (mean ± S.D., $n = 3$) in the lavage fluid.

4. Discussion

The CF loaded DEAPA(39)-10 nanoparticles were prepared by a modified solvent displacement technique. Due to their unique properties, such as biocompatibility and controlled variability of biodegradation rates, the DEAPA polymers are highly suited for pulmonary application (Dailey et al., 2005). Furthermore, their amphiphilic attributes facilitate nanoparticle generation without the requirement of surfactants. The addition of varying amounts of a polyanionic excipient, such as dextrane sulfate or carboxymethyl cellulose (CMC), to the polymer during nanoparticle formulation causes precipitation into highly reproducible nanoparticles with a size of approximately 200 nm in diameter and adjustable physicochemical properties (Dailey et al., 2003a). In this study, CMC, a customary pharmaceutical excipient, was chosen as stabilizer, whose use led to a negative surface charge of the prepared DEAPA(39)-10 nanoparticles. However, the role of CMC may be substituted by any other polyanion, including dextran sulfate, which has been previously used in the pulmonary tract as a mucolytical agent in cystic fibrosis research (Sudo et al., 2000).

Nanoparticle preparation methods, particular the solvent displacement technique, often incur the drawback of poor incorporation of low molecular weight hydrophilic drugs into nanoparticles prepared from hydrophobic polymers, like PLGA. Encapsulation of water soluble drugs is a difficult task, due to the low affinity of the drug compounds to the polymers on the one hand, and the short distances drugs have to cover to diffuse out of the particles on the

Table 3
Final distribution of the fluorescent dye CF for both formulations in the different compartments of the isolated, perfused and ventilated rabbit lung model.

Formulation	Lavage (ng)	Perfusate (ng)	Dripping fluid (ng)	Samples (ng)	Total (ng)
Solution	1093 ± 361	5110 ± 355	436 ± 340	403 ± 23	7042 ± 517
Nanoparticles	878 ± 161	2365 ± 519	495 ± 403	185 ± 74	3923 ± 1127

Values are presented as the mean ± S.D.
$n = 3$ for each formulation.

other hand (Govender et al., 1999; Peltonen et al., 2004). The solvent selection and addition of different excipients to the inner organic phase, like surfactants, was found to improve encapsulation efficiency. Same results were made by manipulating the outer water phase by pH changes or an addition of salts. However, these methods were not feasible for nanoparticles prepared of DEAPA(39)-10 by the solvent displacement method used in this study. Salt addition to the CMC solution led to notable flocculation, resulting in decreased nanoparticle yields (data not shown). We reached high encapsulation efficiencies of approximately 60% for the water soluble model drug CF, whose log *P* (logarithm of the octanol/water partition coefficient) was reported to be −3.45 (Lahnstein et al., 2008), by vigorously mixing together with the DEAPA(39)-10 polymer prior to the nanoparticle preparation process. It has been previously reported that small molecules containing anionic groups can be complexed and encapsulated efficiently via electrostatic interactions with the amino groups attached to the polymer backbone (Wittmar et al., 2006). This concept is also proposed for the CF loaded DEAPA(39)-10 nanoparticles.

The aspect of drug release from pulmonary delivery systems varies according to the used delivery system as well as to the physicochemical properties of the drug. Therefore, the *in vitro* release profile of the CF loaded DEAPA(39)-10 nanoparticle preparations was investigated. A pronounced burst effect was detected in PBS pH 7.4 as release medium. Hence, a second release medium was tested mimicking the composition of the respiratory tract fluid. For this reason Alveofact®, a naturally derived surfactant, was chosen and added to PBS pH 7.4. Neither a difference in curve progression nor a difference in the released amount of CF was seen (Fig. 4). The release rates of drug compounds from nanoparticulate drug delivery systems is thought to be dependent upon desorption of the surfacebound, adsorbed drug, diffusion through the nanoparticle matrix, rate of polymer degradation and a combined process of degradation and diffusion. Thus, diffusion and biodegradation govern the process of drug release (Soppimath et al., 2001). We suppose that the burst effect for CF loaded DEAPA(39)-10 nanoparticles was attributed to two effects. Firstly, the dilution of the nanoparticle suspensions with an excess of PBS pH 7.4 and Alveofact®, respectively, favoured diffusion of the encapsulated dye into the release medium, and secondly, this diffusion was facilitated by distinct swelling of the nanoparticles in aqueous media at 37 °C (J. Sitterberg, personal communication).

As described above, the nanoparticle preparation method allows the generation of nanoparticles with adjustable properties. This attribute was used to design nanoparticle systems with greater stability in the face of shear forces. Dailey et al. (2003a) have investigated the influence of the stabilizer CMC on the nebulization stability of nanoparticles composed of DEAPA polymers. They found out that increasing amounts of CMC led to improved nebulization stability, with an optimum at 50 μg CMC/mg DEAPA utilizing both air jet and ultrasonic nebulizers. This formulation, in contrast to nanoparticles made from polymers more hydrophobic in nature, such as PLGA, was not prone to aggregation during the process of nebulization, as was shown by laser light scattering and AFM images (Dailey et al., 2003b). Recently, a new type of vibrating mesh nebulizers have been commercialized (Dhand, 2002). These nebulizers may overcome the drawbacks of commonly used nebulizers and have been shown to be suitable for delivery of delicate structures such as liposomes (Kleemann et al., 2007). In this study the actively vibrating mesh nebulizer Aeroneb® Professional was used for nebulization. The investigation of nanoparticle formulation stability to the aerosolization process ensued that the characteristics and encapsulation efficiencies were not significantly affected by nebulization. There was only a negligible change in particle size, polydispersity index, ζ-potential and encapsulation efficiency (Table 1). The size measurements gained by PCS were in good agreement with the AFM data (Fig. 3).

The performance of vibrating mesh nebulizers depends strongly on the fluid physicochemical properties. To produce aerosols applicable for deposition in the respiratory bronchioles and alveolar region, density, surface tension, viscosity and ion concentration of the applied fluids have to be considered. Beside the aerosol characteristics other important attributes, like output rate, are also influenced (Ghazanfari et al., 2007). We demonstrated a high aerosol output rate for NaCl 0.9% and the CF solution using the Aeroneb® Professional and suppose this is due to the high ion concentrations present in both liquids. This is in good agreement with the findings of Zhang et al. (2007), who investigated the influence of ion concentration on the output rate of diverse liquids. They were able to increase the aerosol output rate for solutions by an addition of saline. The aerosol output rate for the CF loaded DEAPA(39)-10 nanoparticle formulation was less when compared with NaCl 0.9% and the CF solution, but no statistically significant differences were observed between the sample values. For both CF formulations the duration for nebulization of 3 ml was pleasant. Since the aerodynamic properties, displayed by the MMAD and GSD, are important parameters for the aerosol deposition within the lungs the size distribution of the formulation aerosols was determined by laser diffraction. This method is well established for size analysis of aerosols and has shown good correlation with pulmonary deposition findings (Clark, 1995). The mean MMAD and GSD of the aerosolized saline and both CF formulations were in the range of previously reported magnitudes for other liquids (Zhang et al., 2007; Lahnstein et al., 2008). Although statistically significant, the differences in the values for MMAD and GSD between NaCl 0.9% and the two formulations are negligible regarding pulmonary deposition. In addition, we investigated the particle size distribution of NaCl 0.9% at the entrance of the inspiratory tubing system to the trachea of the lung. The MMAD decreased significantly by approximately 2 μm (the GSD by approximately 0.4), due to evaporation of liquid from the aerosol droplets and impaction and sedimentation of larger aerosol droplets in the tubing system of the IPL ($p < 0.005$). The aerodynamic properties of the generated aerosol entering the isolated rabbit lung were well suitable for deposition in terminal respiratory bronchioles and in the alveolar region (Raabe et al., 1977). In fact, after inhalative administration of ^{99m}Tc-enriched saline to the IPL a high, reproducible pulmonary deposition was achieved.

In a previous study the authors have compared the chemical properties of three structurally diverse fluorescent probe molecules and investigated the pulmonary absorption and distribution following their inhalative intrapulmonary administration in an IPL (Lahnstein et al., 2008). They concluded that CF is a suitable model drug for the examination of pulmonary drug delivery formulations in an IPL. Therefore CF was chosen as a water soluble model drug and encapsulated in nanoparticles composed of DEAPA(39)-10. As expected by the promising results from *in vitro* (Unger et al., 2007) and *in vivo* toxicological studies (Dailey et al., 2006), after nebulization of nanoparticles to the IPL the lungs fulfilled the three claimed criteria. During the whole experiment they maintained homogeneous white appearance with no signs of haemostasis, oedema, or atelectasis; a pulmonary artery and ventilation pressure in the normal range; and isogravimetry. Regarding the lung architecture, there are only very small amounts of liquid at the respiratory site. Thus, we expected that the burst effect, which occurred upon dilution with release medium, would not be found after aerosolization of the nanoparticle suspensions to the IPL. Indeed, the CF absorption by the IPL from CF loaded DEAPA(39)-10 nanoparticles was less compared to the absorption after deposition of the same amount of

CF aerosolized as solution denoted by a lower plateau concentration in the perfusate (Table 2, Fig. 6). If the burst would have occurred to the same extent as found during the *in vitro* release, the perfusate concentrations following application of CF loaded nanoparticles would have hardly differed from those of CF absorbed from the solution. Thus, we suppose that due to the smaller liquid volume in the lung, the burst effect was reduced. On the other hand, the concentration in the perfusate was higher as expected by the absorption of unencapsulated CF only. Hence, the free unencapsulated CF and a small amount of CF released from the CF loaded nanoparticles were absorbed by the IPL and appeared in the perfusate. This idea is in agreement with the estimated MRT of CF for both formulations in the lung. Empirical distribution functions are characterized by their statistical moments, e.g. MRT. The increase in perfusate concentration over the time is due to absorption of released drug from the administered formulation. The MRT, as defined by Dost (1958), is the arithmetic mean of individual absorption times of drug released from its formulation. Similar formulations yield similar MRT values. This was the case for the two formulations used in this study with regard to curve progression. The nanoparticle formulation resulted in a slightly higher MRT value compared with the solution, denoting absorption of free unencapsulated CF and a small amount of CF that has been released from the CF loaded nanoparticles by the IPL. We suppose that nanoparticles either reached the interstitial spaces or were internalized into lung cells. The localization in the interstitial spaces led to a dilution of the nanoparticle suspensions, resulting in release of CF from the nanoparticles. From there it could be readily adsorbed by pore diffusion and osmotically driven processes, as described previously (Pohl et al., 1998, 1999). Dailey et al. investigated the cell association and internalization of nanoparticles of the same type as used in this study *in vitro* with the alveolar epithelial cell line A549 (Dailey et al., 2003a). Nanoparticle internalization could be detected by confocal laser scanning fluorescence microscopy (CLSFM). The distribution of CF in the different compartments of the IPL (Table 3) was in good agreement with this observation. Compared to the distribution pattern of free CF, those of CF from nanoparticles differed. While the recovered CF applied as solution was approximately 7.0 μg from the different compartments of the IPL, only 3.9 μg of the CF from the nanoparticle suspensions were found. Assuming the localization of nanoparticles in the interstitial spaces, lavage would have led to release of CF from the carriers upon dilution and an increased amount of CF would have been found in the lavage fluid. But this was not the case. The decreased total recovery of only 56% for the CF from nanoparticles compared to the total recovery for free CF, might have been attributed to internalization of nanoparticles into lung cells, hence not recovered during lavage. The localization of DEAPA(39)-10 nanoparticles as well as entrapped and free CF in different cell types and lung regions after their administration to the IPL was investigated by CLSFM. Unfortunately, the strong green autofluorescence of the lung tissue superimposed the fluorescence signals of CF. However, alternative effects, which might have led to the reported concentration–time profiles and dye recovery, have to be considered. The interaction of the nanoparticles with surfactant components and lung cells are only two examples of a magnitude of possibilities. Thus, more sophisticated *in vitro* investigations accounting for the fluid composition and volumes that can be found in the respiratory space, as well as studies on the localization of the nanoparticles in lung cells and in different lung compartments after aerosol application are indicated to fully explain the absorption pattern reported in this study. Currently, experiments to localize nanoparticles as well as drug within the lung and mechanistic studies concerning their uptake into lung cells are under investigation using different techniques, such as quantum dots and will be reported elsewhere.

In conclusion, this study showed that the solvent displacement method is feasible to encapsulate hydrophilic drugs into polymeric nanoparticles. High encapsulation efficiencies of the model drug CF were reached using the biocompatible, fast degrading, branched polyester DEAPA(39)-10. *In vitro* release studies showed a distinct burst release of the encapsulated CF. Investigation of nanoparticle formulation stability to the aerosolization process utilizing the Aeroneb® Professional ensured that the characteristics and encapsulation efficiencies were not affected by nebulization. The aerodynamic properties of the generated aerosol droplets, displayed by the MMAD and GSD at the entrance of the inspiratory tubing system to the trachea of the lung, were suitable for alveolar deposition. In fact, after inhalative administration of both formulations to the IPL, CF showed a reproducible pulmonary absorption with a stable concentration plateau in the perfusate. The perfusate concentration–time profiles exhibited similar characteristics with regard to the curve progression. But the absorption degree of CF released from nanoparticles by the IPL was less than those of CF solution denoted by a lower concentration plateau in the perfusate. Thus, burst release in the IPL was supposed to occur to a lesser extent than *in vitro*. The amount of CF that remained in the other compartments of the IPL was similar for both formulations indicating a distribution of the CF loaded nanoparticles into the lung tissue. Further investigations to characterize the behaviour of nanoparticles at the air/blood interface, the localization of nanoparticles as well as entrapped and free drug in different cell types and lung regions after their administration need to be carried out.

Acknowledgements

The authors would like to thank Johannes Sitterberg (Department of Pharmaceutical Technology and Biopharmaceutics, University of Marburg) for his support with AFM and Nadine Faulstich (Medical Clinic II, Department of Internal Medicine, Justus-Liebig-University Giessen) for her technical assistance.

This study is part of the research project "Polymeric nano-carrier for pulmonary drug administration (Nanohale, FOR 627)" which is supported by the German Research Foundation (DFG). We want to express our sincere thanks for this grant.

References

Azarmi, S., Roa, W.H., Loebenberg, R., 2008. Targeted delivery of nanoparticles for the treatment of lung diseases. Adv. Drug Del. Rev. 60, 863–875.

Badesch, D.B., Abman, S.H., Ahearn, G.S., Barst, R.J., McCrory, D.C., Simonneau, G., McLaughlin, V.V., 2004. Medical therapy for pulmonary arterial hypertension. ACCP evidence-based clinical practice guidelines. Chest 126, 35S–62S.

Clark, A.R., 1995. The use of laser diffraction for the evaluation of the aerosol clouds generated by medical nebulizers. Int. J. Pharm. 115, 69–78.

Dailey, L.A., Kleemann, E., Wittmar, M., Gessler, T., Schmehl, T., Roberts, C., Seeger, W., Kissel, T., 2003a. Surfactant-free, biodegradable nanoparticles for aerosol therapy based on branched polyesters, DEAPA-PVAL-*g*-PLGA. Pharm. Res. 20, 2011–2020.

Dailey, L.A., Schmehl, T., Gessler, T., Wittmar, M., Grimminger, F., Seeger, W., Kissel, T., 2003b. Nebulization of biodegradable nanoparticles: impact of nebulizer technology and nanoparticle characteristics on aerosol features. J. Controlled Rel. 86, 131–144.

Dailey, L.A., Wittmar, M., Kissel, T., 2005. The role of branched polyesters and their modifications in the development of modern drug delivery vehicles. J. Controlled Rel. 101, 137–149.

Dailey, L.A., Jekel, N., Fink, L., Gessler, T., Schmehl, T., Wittmar, M., Kissel, T., Seeger, W., 2006. Investigation of the proinflammatory potential of biodegradable nanoparticle drug delivery systems in the lung. Toxicol. Appl. Pharmacol. 215, 100–108.

Dhand, R., 2002. Nebulizers that use a vibrating mesh or plate with multiple apertures to generate aerosol. Resp. Care 47, 1406–1416.

Dost, F.H., 1958. Ueber ein einfaches statistisches Dosis-Umsatz-Gesetz. Klin. Wschr. 36, 655–657.

Ewing, P., Blomgren, B., Ryrfeldt, A., Gerde, P., 2006. Increasing exposure levels cause an abrupt change in the absorption and metabolism of acutely inhaled benzo(*a*)pyrene in the isolated, ventilated, and perfused lung of the rat. Toxicol. Sci. 91, 332–340.

Ewing, P., Eirefelt, S.J., Andersson, P., Blomgren, A., Ryrfeldt, A., Gerde, P., 2008. Short inhalation exposures of the isolated and perfused rat lung to respirable dry particle aerosols; the detailed pharmacokinetics of budesonide, formoterol, and terbutaline. J. Aerosol Med. 21, 169–180.

Gessler, T., Schmehl, T., Hoeper, M.M., Rose, F., Ghofrani, H.A., Olschewski, H., Grimminger, F., Seeger, W., 2001. Ultrasonic versus jet nebulization of iloprost in severe pulmonary hypertension. Eur. Respir. J. 17, 14–19.

Gessler, T., Schmehl, T., Seeger, W., 2008. Inhaled prostanoids in the therapy of pulmonary hypertension. J. Aerosol Med. 21, 1–12.

Ghazanfari, T., Elhissi, A.M.A., Ding, Z., Taylor, K.M.G., 2007. The influence of fluid physicochemical properties on vibrating-mesh nebulization. Int. J. Pharm. 339, 103–111.

Govender, T., Stolnik, S., Garnett, M.C., Illum, L., Davis, S.S., 1999. PLGA nanoparticles prepared by nanoprecipitation: drug loading and release studies of a water soluble drug. J. Controlled Rel. 57, 171–185.

Jung, T., Breitenbach, A., Kissel, T., 2000. Sulfobutylated poly(vinyl alcohol)-*graft*-poly(lactide-*co*-glycolide)s facilitate the preparation of small negatively charged biodegradable nanospheres. J. Controlled Rel. 67, 157–169.

Kleemann, E., Schmehl, T., Gessler, T., Bakowsky, U., Kissel, T., Seeger, W., 2007. Iloprost-containing liposomes for aerosol application in pulmonary arterial hypertension: formulation aspects and stability. Pharm. Res. 24, 277–287.

Lahnstein, K., Schmehl, T., Ruesch, U., Rieger, M., Seeger, W., Gessler, T., 2008. Pulmonary absorption of aerosolized fluorescent markers in the isolated rabbit lung. Int. J. Pharm. 351, 158–164.

McLaughlin, V.V., Shillington, A., Rich, S., 2002. Survival in primary pulmonary hypertension. The impact of epoprostenol therapy. Circulation 106, 1477–1482.

Olschewski, H., Simonneau, G., Galiè, N., Higenbottam, T., Naeije, R., Rubin, L.J., Nikkho, S., Speich, R., Hoeper, M.M., Behr, J., Winkler, J., Sitbon, O., Popov, W., Ghofrani, H.A., Manes, A., Kiely, D.G., Ewert, R., Meyer, A., Corris, P.A., Delcroix, M., Gomez-Sanchez, M., Siedentop, H., Seeger, W., Aerosolized Iloprost Randomized Study Group, 2002. Inhaled iloprost for severe pulmonary hypertension. N. Engl. J. Med. 347, 322–329.

Peltonen, L., Aitta, J., Hyvoenen, S., Karjalainen, M., Hirvonen, J., 2004. Improved entrapment efficiency of hydrophilic drug substance during nanoprecipitation of poly(L)lactide nanoparticles. AAPS Pharm. Sci. Tech. 5, 16, article.

Pison, U., Welte, T., Giersig, M., Groneberg, D.A., 2006. Nanomedicine for respiratory diseases. Eur. J. Pharmacol. 533, 341–350.

Pohl, R., Kramer, P.A., Thrall, R.S., 1998. Confocal laser scanning fluorescence microscopy of intact unfixed rat lungs. Int. J. Pharm. 168, 69–77.

Pohl, R., Thrall, R.S., Rogers, R.A., Kramer, P.A., 1999. Confocal imaging of peripheral regions of intact rat lungs following intratracheal administration of 6-carboxyfluorescein, FITC-insulin, and FITC-dextran. Pharm. Res. 16, 327–332.

Raabe, O.G., Yeh, H.-C., Newton, G.J., Phalen, R.F., Velasquez, D.J., 1977. Deposition of inhaled monodisperse aerosols in small rodents. In: Walton, W.H. (Ed.), Inhaled Particles IV. Pergamon Press, Oxford, pp. 3–21.

Rich, S., McLaughlin, V.V., 1999. The effects of chronic prostacyclin therapy on cardiac output and symptoms in primary pulmonary hypertension. J. Am. Coll. Cardiol. 34, 1184–1187.

Rytting, E., Nguyen, J., Wang, X., Kissel, T., 2008. Biodegradable polymeric nanocarriers for pulmonary drug delivery. Exp. Opin. Drug Deliv. 5, 629–639.

Sakagami, M., 2006. In vivo, in vitro and ex vivo models to assess pulmonary absorption and disposition of inhaled therapeutics for systemic delivery. Adv. Drug Del. Rev. 58, 1030–1060.

Seeger, W., Walmrath, D., Grimminger, F., Rosseau, S., Schuette, H., Kraemer, H.-J., Ermert, L., Kiss, L., 1994. Adult respiratory distress syndrome: model systems using isolated perfused rabbit lungs. Methods Enzymol. 233, 549–584.

Soppimath, K.S., Aminabhavi, T.M., Kulkarni, A.R., Rudzinski, W.E., 2001. Biodegradable polymeric nanoparticles as drug delivery devices. J. Controlled Rel. 70, 1–20.

Sudo, E., Boyd, W.A., King, M., 2000. Effects of dextran sulfate on tracheal mucociliary velocity in dogs. J. Aerosol Med. 13, 87–96.

Sung, J.C., Pulliam, B.L., Edwards, D.A., 2007. Nanoparticles for drug delivery to the lungs. Trends Biotechnol. 25, 563–570.

Unger, F., Wittmar, M., Kissel, T., 2007. Branched polyesters based on poly[vinyl-3-(dialkylamino)alkylcarbamate-*co*-vinyl acetate-*co*-vinyl alcohol]-*graft*-poly(D,L-lactide-*co*-glycolide): effects of polymer structure on cytotoxicity. Biomaterials 28, 1610–1619.

Unger, F., Wittmar, M., Morell, F., Kissel, T., 2008. Branched polyesters based on poly[vinyl-3-(dialkylamino)alkylcarbamate-*co*-vinyl acetate-*co*-vinyl alcohol]-*graft*-poly(D,L-lactide-*co*-glycolide): effects of polymer structure on in vitro degradation behaviour. Biomaterials 29, 2007–2014.

Wittmar, M., Unger, F., Kissel, T., 2006. Biodegradable brushlike branched polyesters containing a charge-modified poly(vinyl alcohol) backbone as a platform for drug delivery systems: synthesis and characterization. Macromolecules 39, 1417–1424.

Yang, W., Peters, J.I., Williams III, R.O., 2008. Inhaled nanoparticles—a current review. Int J. Pharm. 356, 239–247.

Zeng, X.M., Martin, G.P., Marriott, C., 1995. The controlled delivery of drugs to the lung. Int. J. Pharm. 124, 149–164.

Zhang, G., David, A., Wiedmann, T.S., 2007. Performance of the vibrating membrane aerosol generation device: aeroneb micropump nebulizer™. J. Aerosol Med. 20, 408–416.